Thermal Stresses on a Reginal Cooling Plate

Ibrahim Koc*‡

*Department of Aircraft Fuselage-Engine Maintenance, School of Applied Sciences, Istanbul Gelisim University, 34215 Istanbul, Turkey

(ibkoc@gelisim.edu.tr)

‡Corresponding Author; Ibrahim Koc, Department of Aircraft Fuselage-Engine Maintenance, School of Applied Sciences, Istanbul Gelisim University, 34215 Istanbul, Turkey, Tel: +90 212 422 7020, Fax: +90 212 422 7401, ibrahimkoc4951@gmail.com

Abstract- In this study, stresses and strains that occur on the surface of material are investigated for a flat plate that is made cooling as numerically and analytically. The cooling blowing ratios applied to the surface vary between 0.5 and 1.75. The cooling injection angle is 30 degrees with the horizontal. Plexiglas plate were used in experiments which done for analytical solution and numerical modelling studies. Air was injected to cooling zone at 57 ºC and 77 ºC. The results show that the cooling surface size varies with the blow ratio. In addition, the sizes of thermal stresses and displacements of surface set out that they are indicators of cooling.

Keywords Cooling, thermal stress, cooled plate.

1. Introduction

Generally, the formation of any temperature gradient along the wall of a container causes thermal stress. Detailed thermal stress analysis for spherical and cylindrical containers is given [1-4].

Composite materials, which are made of ceramics and metals, are already used in heat resistant parts, such as pistons. Functionally gradient materials (FGM) are composite materials. They reduce the thermal stress and they are resistant to super high temperature. In order to support the design of FGM, the computer programs that analyses the transient heat transfer and the transient thermal stress of FGM have developed [5]. The finite element method is used in this study.

Application of Taylor transformation to the thermal-stresses in isotropic annular fins presents the stresses distribution in a perfectly elastic isotropic annular fin. The stresses distribution is integrated obtain the results. The thickness of the fins is assumed sufficiently small so as to have a state of plane stress and one-dimensional heat conduction [6]. "A coupled heat transfers and thermal stress analysis is developed for a thin-film high Tc superconductor device" [7]. The stress fields in the adhesive layer and the composite members of two tee joints bonded to a rigid base and a flexible plate were investigated [8].

In this study, the inclined jet was applied on the Plexiglas plate. Stress and strain in the material were investigated numerically and analytically.

2. Experimental Apparatus and Procedure for Analytical Solution

A schematic view of wind tunnel used in the experiments which done for analytical solution is presented in Figure 1. The test set up consists of a fan, heater, orifice, plenum chamber, Plexiglas plate, thermocouple, hot-wire anemometry, miniature wire probe (55P15), probe support for single-sensor probe, traverse system and computer. The test section is 460 mm wide, 460 mm high and 610 mm long. The blowing ratios are 0.50, 0.75, 1.0, 1.25, 1.50, 1.75 and the injection angle with respect to the horizontal plane is 30º.
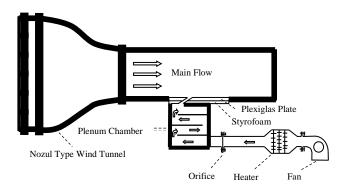

Fig. 1. Schematic view of test facility.

In the experiments, a transparent Plexiglas plate with a small conduction coefficient is used. A plenum chamber is used to supply a steady injection. The orifice made of Plexiglas was designed to measure the flow rate of injected

air. Centrifugal fan for injection of air from out to the test chamber and the heater for getting up the ambient temperature to 330 K and 350 K and a rheostat for controlling the power of heater are used. The heater has two resistances and both of them are 1000 W. Oblique manometer for calculating mass flux of air, which is injected, and the insulation material which is 5 mm thickness for preventing the heat losses from Plexiglas surface to the surroundings are used. In addition, digital thermometer and the thermocouples which are K (Chromel-Alumel) type for measuring of temperature also the cardboards for getting different mass fluxes in experiments are used.

Eleven injection holes in a single row are located on a Plexiglas plate for thermal stress and strain investigation. The hole's cross-section diameters are 8.5 mm. All of the hole geometries in the model are cylindrical and they have the same cross-section area value. The injection angles are 30° to the surface and main flow. Measurements were made for cylindrical holes at the exit of the sixth hole. Schematic view of cylindrical holes is presented in Figure 2. The place of the coordinate axes was considered as out of the sixth hole.
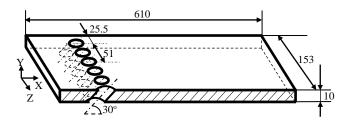

Fig. 2. Schematic view of cylindrical holes with a row.

Plexiglas plate was fastened the wind tunnel test room's surface as shown Figure 3. In order to measure the temperature of Plexiglas surface, thermocouples were fitted to the surface. The position of the thermocouples, K type, is shown Figure 3.
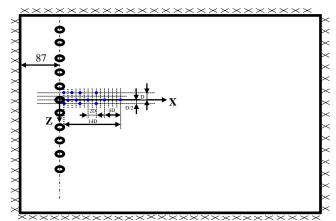

Fig. 3. The position of thermocouples on the Plexiglas plate.

In the experiments, the warmer air from the main flow air is injected into the wind tunnel at an angle of 30 degrees. The main flow velocity is measured by using hot wire probe 55P11 (Dantec hot-wire probe). The injection velocities are used for the calculations of blowing ratios. These velocity values were found by using orifice. The suitable velocities were regulated by using the cardboards that are attached on the fan. Hot-wire anemometry is used for the measurement of velocity in single dimension. This device is also called Constant-Temperature Anemometer (CTA). The measurement probe is calibrated in the wind tunnel before the measurement of velocity is experimented. The velocity values, 0, 5, 10, 15, 20, 25 and 30 m/s, were considered for calibration. The traverse system is used for moving the probe to a known point. The computer is used for analyzing the data obtained from the hot wire anemometry.

Measurements were done for cylindrical holes. The air is injected 57 °C and 77 °C. The blowing ratios are 0.50, 0.75, 1.00, 1.25, 1.50 and 1.75. The injection velocity is used for the calculation of blowing ratio. This velocity value was found by using orifice. Data used in measurements are given in Table 1.

Table 1. The values used to measure blowing ratio

Hole geometry	The injection air				The main flow characteristics				
	T_j(K)	V_j(m/s)	ρ_j(kg/m³)	$\dot{m}$ (kg/s)	T_∞(K)	V_∞(m/s)	ρ_∞(kg/m³)	M	I
		6.17		0.0041	298.5		1.1845	0.50	0.295
		9.26		0.0061	296.4		1.1943	0.75	0.659
	330	12.34	1.0516	0.0082	298.5	10.70	1.1845	1.00	1.180
		15.43		0.0102	297.3		1.1901	1.25	1.837
		18.51		0.0123	298.9		1.1826	1.50	2.660
Cylindrical		21.60		0.0143	296.9		1.1920	1.75	3.470
		6.35		0.0039	298.6		1.1840	0.50	0.317
		12.69		0.0079	298.9		1.1826	1.00	1.271
	350	15.86	0.9980	0.0099	298.2	10.34	1.1859	1.25	1.979
		19.04		0.0119	298.2		1.1859	1.50	2.853
		22.21		0.0138	298.2		1.1859	1.75	3.882

The mainstream air velocity and the injected air velocity ratio are determined according to the blowing ratio:

$$M = \frac{\rho_j V_j}{\rho_\infty V_\infty} \tag{1}$$

Where M is the blowing ratio, is the injected fluid density, is the injected fluid velocity, is the main flow density and is the main flow velocity. The injected cooling air temperature was selected as 330 and 350 K.

One of the parameters that affect the flow field is the momentum flux ratio. The momentum flux ratio is used as some physical justification for choosing the blowing ratio. It is well accepted that the key parameter of jet penetration in a cross flow is the momentum flux ratio, shown in equation 2. In the experiments, the different momentum fluxes are obtained by changing the temperature of the injected air. The momentum flux ratio is determined by as follows [9]:

$$I = \frac{\rho_j V_j^2}{\rho_\infty V_\infty^2} \tag{2}$$

Where I is the momentum flux ratio. The values of momentum flux ratio are given in table 1.

The hot air which is 330 K is injected into the main flow which is about 10.70 m/s velocity. The hot air which is 350 K is injected into the main flow which is about 10.34 m/s velocity. In experiments, the temperatures on the Plexiglas plate were measured for the second hole in different mass fluxes by using thermocouples. The thermal stress and strain was calculated from measuring temperatures.

The ambient temperature is heated in the heater and then it is forwarded to the plenum chamber and it is exerted to pressure in plenum chamber and it is injected into the main flow for injection holes which are 30º to the main flow.

The temperature of the air which is injected from holes and the temperature of main flow should be known for calculations of thermal stress and strain. Therefore, one apiece number thermocouples are located to the entering of Plexiglas in the wind tunnel.

In analytical solutions, the thermal stresses and strains variations on cooled plate which is made of Plexiglas material are investigated for the different blowing ratios which are defined in top. The 2D thermal stress field was calculated for different blowing ratios at flat surface. The thermal stress was calculated from temperatures using the following equation:

$$\sigma = \alpha \Delta T E \tag{3}$$

$$\alpha = \frac{1}{L} \frac{\Delta L}{\Delta T} \tag{3.1}$$

Where σ is the stress, α is the coefficient linear thermal expansion, ΔT is temperature difference, E is the modulus of elasticity, L is the length of material and ΔL is the elongation. In the analytical solution and numerical study the modulus of elasticity (E) and the coefficient linear thermal

expansion (α) were taken 3.102·10³ N/mm² [10] and 7.5·10⁻⁵ [11] respectively.

3. Numerical Investigation

Computations are performed to simulate thermal stresses over the cooled plate. The 3D computational domain is shown in Figure 4. GAMBIT software [12-15] was used to create the geometry and related mesh for the domain. A commercial CFD code based upon finite element volume, FLUENT 5.4 [12-15] has been applied to the flow simulation.
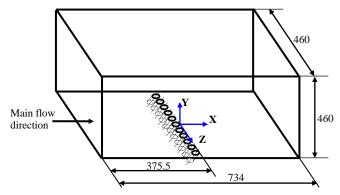

Fig. 4. Schematic view of the wind tunnel model.

Tetrahedral mesh for the injection holes and hexahedral mesh for the rest of the domain were used. The injection holes were finer meshed compared to other sections. Standard k-ε turbulence model [16] and standard wall function [17] are employed. The standard k-ε model is a semi-empirical model and it is based on model transport equations for the turbulent kinetic energy (k) and its dissipation rate (ε). The model transport equation for k is derived from the exact equation, while the model transport equation for ε is obtained using physical reasoning and bears little resemblance to its mathematically exact counterpart. In the derivation of the k-ε model, it was assumed that the flow is fully turbulent and the effects of molecular viscosity are negligible. The wall function is used between the turbulent zone and the wall. Therefore, the distance from the wall at the cells adjacent to the wall was determined by considering the range over which the log law is valid.

The distance, which is between the best adjacent mesh and the surface, was considered. Non-dimensional numbers were defined [18]:

$$y^+ = \frac{Y u^*}{\upsilon} \tag{4}$$

$$u^* = \frac{U}{u^+} \tag{4a}$$

$$u^+ = \frac{1}{\kappa} \ln E y^+ \tag{4b}$$

In equation (4), u* is frictional velocity, is non-dimensional length, is non-dimensional velocity, U is the flow velocity and is von Karman constant, where κ is 0.4

and E is 9. y^+ is less than 10 value in the laminar zone. The turbulence models are not used at this zone. In generally, is recommended from 20 to 50 values. The suitable y^+ value was selected from 30 to 40 in numerical study.
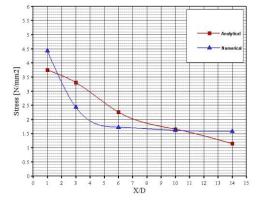
The assumptions were as follows in numerical study. Heat loss from the injection holes' surfaces is not there and the system is steady state. The air is an ideal gas and it is compressible. In addition, radiation and conduction are neglected. The turbulence intensity for the main stream, for the jets entering the computation domain and for backflow is taken as 1 per cent.

In numerical study, the injected cooling air velocity and related temperature, the mainstream air velocity and related temperature were taken from the experiments.

4. Results and Discussion

The following results are found for the effects of blowing ratios and temperatures on the thermal stresses and the displacements of surface as analytical and numerical. The experiments which done for analytical solution were done at the injection temperature that are 330 and 350 K and the main flow temperature, which is ambient temperature. The experiments were carried out for with the blowing ratios and temperatures. The stress in main flow direction were evaluated for z/D = 0 at 330 K (Figures 5-10) and 350 K (Figures 11-15).

When the figures are investigated, the stress is high value in low-blowing ratios (Figures 5-10). The biggest stress is 0.5 in the present blowing ratios as shown in Figures 5-10. For example, in Figure 5, the stress is 4.4290 N/mm² for the numerical study at X/D = 1 at the 0.5 blowing ratio and in Figure 6 and Figure 7 and Figure 8 and Figure 9 and Figure 10, the stresses are 3.9342 N/mm² and 3.0555 N/mm² and 2.4912 N/mm² and 1.9171 N/mm² and 2.0474 N/mm² at the 0.75 and 1.00 and 1.25 and 1.50 and 1.75 blowing ratio in the same point, respectively. For the analytical study at X/D = 1 at the 0.5 blowing ratio, the stress is 3.7464 N/mm² in Figure 5. In Figure 6 and Figure 7 and Figure 8 and Figure 9 and Figure 10, the stresses are 3.4672 N/mm² and 3.1414 N/mm² and 2.2572 N/mm² and 2.7109 and 2.5248 N/mm² at the 0.75 and 1.00 and 1.25 and 1.50 and 1.75 blowing ratio in the same point, respectively. A similar situation can be seen in the figures in different points (Figures 5-10). From these results, the cooling surface is better at the 0.5 blowing ratio.

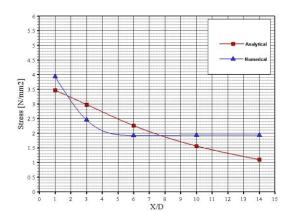**Fig. 5.** The stress in the main flow direction for M=0.5(Z=0)

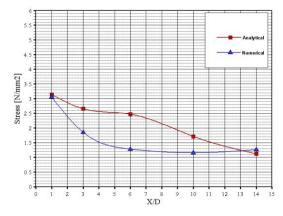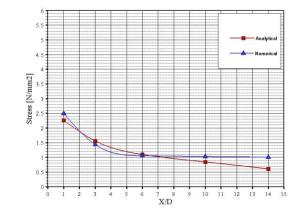**Fig.6.** The stress in the main flow direction for M=0.75(Z=0)

Fig.7. The stress in the main flow direction for M=1.00(Z=0)

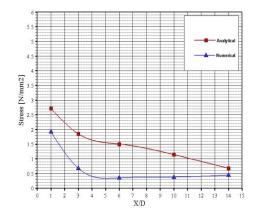**Fig.8.** The stress in the main flow direction for M=1.25(Z=0)

Fig.9. The stress in the main flow direction for M=1.50(Z=0)
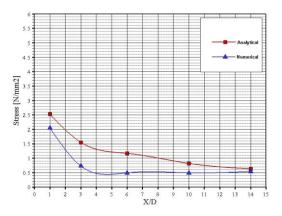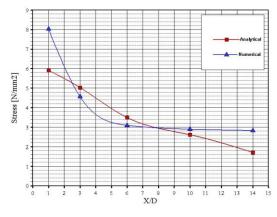
Fig.10. The stress in the main flow direction for M=1.75(Z=0)

When the differences between the injection temperature and main flow temperature are increased the stress increases for the same blowing ratios in mainstream direction (Figures 11-15). For example, in Figure 5, while the stress is 4.4290 N/mm² and 3.7464 N/mm² for 330 K injection temperature at X/D = 1 at the 0.5 blowing ratio, in Figure 11, the stress is 8.0220 N/mm² and 5.9105 N/mm² for 350 K injection temperature in the same point and the same blowing ratio.

Especially, this situation is seen in the high-blowing ratios as shown in Figure 10 and 15. For example, the maximum stress values are 2.0474 N/mm² and 2.5248 N/mm² for 1.75 blowing ratio at 330 K injection temperature (Figure 10) but they are 3.6360 N/mm² and 4.1420 N/mm² for the same blowing ratio at 350 K injection temperature (Figure 15).

The results of numerical and analytical studies were given for blowing ratios as similar comparing from figure 5 to figure 15. When the blowing ratio is increased, the stress decreases in both numerical and analytical studies for the main flow direction (Figures 5-15).

When the analytical and numerical studies were investigated their results are in good agreement each other as seen in Figures 5-15. The deviations of the numerical studies can result from the insufficiency of turbulence modelling in mixture part and from the wall function and from the assumptions.

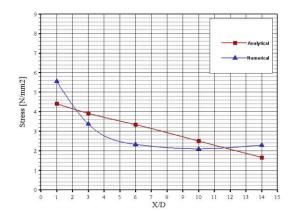**Fig.11.** The stress in the main flow direction for M = 0.5 (Z=0)

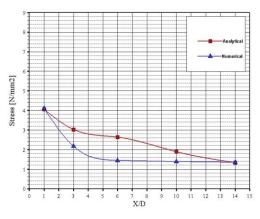**Fig.12.** The stress in the main flow direction for M=1.00(Z=0)

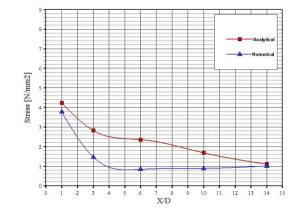**Fig.13.** The stress in the main flow direction for M=1.25(Z=0)

Fig.14. The stress in the main flow direction for M=1.50(Z=0)
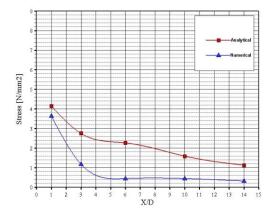

Fig.15. The stress in the main flow direction for M=1.75(Z=0)

The results of measuring of strain on the flat surface show that the value of strain is bigger in the low blowing ratios (Figures 16-21). It is difficult to bend the injection coming from holes at the high blowing ratios. Moreover, there are more separations from the surface at the high blowing ratios. Therefore, the high strain exists near the hole regions for the low blowing ratios.

For example, in Figure 16, the strain is 856.50 μm for the numerical study at X/D = 1 at the 0.5 blowing ratio and in Figure 17 and Figure 18 and Figure 19 and Figure 20 and Figure 21, the strains are 760.81 μm and 590.89 μm and 481.76 μm and 370.73 μm and 395.93 μm at the 0.75 and 1.00 and 1.25 and 1.50 and 1.75 blowing ratio in the same point, respectively. For the analytical study at X/D = 1 at the 0.5 blowing ratio, the strain is 724.50 μm in Figure 16. In Figure 17 and Figure 18 and Figure 19 and Figure 20 and Figure 21, the strains are 670.50 μm and 607.50 μm and 436.50 μm and 524.25 μm and 488.25 μm at the 0.75 and 1.00 and 1.25 and 1.50 and 1.75 blowing ratio in the same point, respectively. A similar situation can be seen in the figures in different points (Figures 16-21). From these results, the strain on the cooling surface is bigger at the 0.5 blowing ratio.
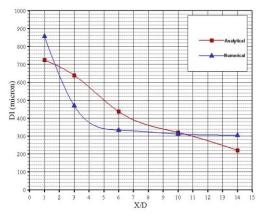

Fig.16. The strain in the main flow direction for M = 0.50 (Z = 0)
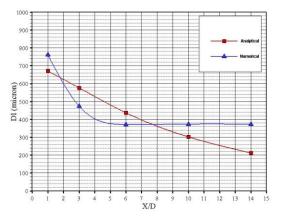

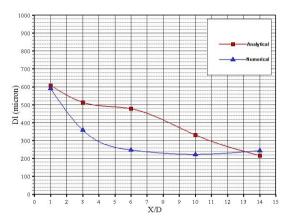**Fig.17.** The strain in the main flow direction for M = 0.75 (Z = 0)

Fig.18. The strain in the main flow direction for M = 1.00 (Z = 0)
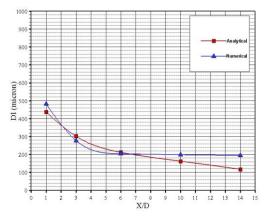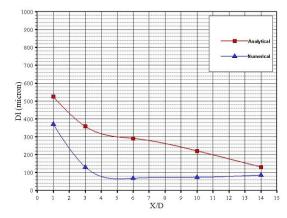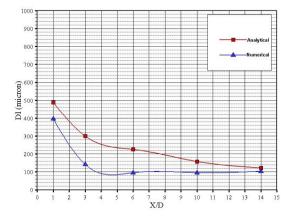

Fig.19. The strain in the main flow direction for M = 1.25 (Z = 0)

Fig.20. The strain in the main flow direction for M = 1.50 (Z = 0)
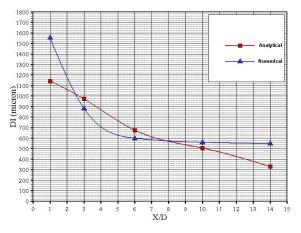

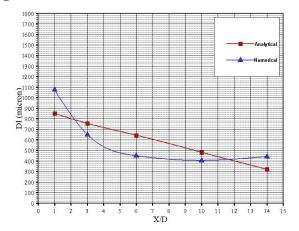**Fig.21.** The strain in the main flow direction for M = 1.75 (Z = 0)

When the differences between the injection temperature and main flow temperature are increased the strain increases for the same blowing ratios in mainstream direction (Figures 16, 22). For example, in Figure 16, while the strains are 856.50 μm and 724.50 μm for 330 K injection temperature at X/D = 1 at the 0.5 blowing ratio, in Figure 22, the strains are 1551.32 μm and 1143.00 μm for 350 K injection temperature in the same point and the same blowing ratio.

The results of numerical and analytical studies were given for blowing ratios as similar comparing from figure 22 to figure 26. When the blowing ratio is increased, the strain decreases in both numerical and analytical studies for the main flow direction (Figures 22-26).

When the analytical and numerical studies were investigated their results are in good agreement each other as seen in Figures 22-26. The deviations of the numerical studies can result from the insufficiency of turbulence modelling in mixture part and from the wall function and from the assumptions.

Fig.22. The strain in the main flow direction for M = 0.50 (Z = 0)

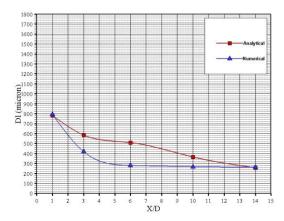**Fig.23.** The strain in the main flow direction for M = 1.00 (Z = 0)

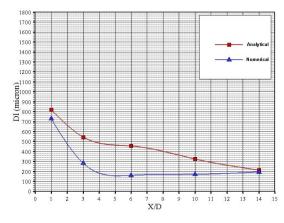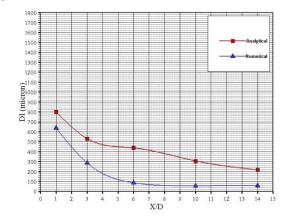**Fig.24.** The strain in the main flow direction for M = 1.25 (Z = 0)

Fig.25. The strain in the main flow direction for M = 1.50 (Z = 0)

Fig.26. The strain in the main flow direction for M = 1.75 (Z = 0)

5. Conclusion

In this study, stresses and strains which occur on the surface of material are investigated for a flat plate which is made cooling as numerically and analytically. As on conclusions following results are found:

• the blowing ratio and injection temperature affect the stress and strain on cooled flat;

• the stress and strain are reduced in main flow direction;

• for stress and strain, the biggest values are blowing ratio 0.5 in the main flow direction;

• when the blowing ratio is increased the stress and strain decrease in main flow direction;

• when the difference between the injection and main flow temperature is increased the stress and strain increase in main flow direction;

• the value of cooling effectiveness is better in the low blowing ratios;

• the stress and strain are higher in the region close to the hole because of the jet impact;

• the penetration of the jets which have low blowing ratios into the main flow is better than the others;

the stress and strain decrease away from the jet holes.

References

[1] S. Timoshenko and J.N. Goodier, Theory of Elasticity, McGraw-Hill, New York, 1951.

[2] B. A. Boley and J. Fr. Weiner, Theory of Thermal Stresses, Wiley, New York, 1960.

[3] W. Nowaki, Thermo-Elasticity, Pergamon Press, Oxford, 1965.

[4] W. Johnson and P.B. Mellor, Engineering Plasticity, Ellis Harwood, London, 1983.

[5] T. Fuchiyama and N. Noda, "Analysis of Thermal Stress in a Plate of Functionally Gradient Material", The Society of Automotive Engineers of Japan, vol. 16, No.3, pp. 263-268, 1995.

[6] L.T. Yu and C.K. Chen, "Application of Taylor Transformation to the Thermal Stresses in Isotropic Annular Fins", J. Therm. Stresses., vol.21, No.8, pp. 781-809, 1998.

[7] B. Gu, P.E. Phelan and S. Mei, "Coupled Heat Transfer and Thermal Stress in High-t-c Thin-Film Superconductor Devices", Cryogenics, vol. 38, No.4, pp. 411-418, 1998.

[8] M.K. Apalak, Z.G. Apalak and R. Gunes, "Thermal and Geometrically Nonlinear Stress Analyses of an Adhesively Bonded Composite Tee Joint with Double Support", J. Thermoplast. Compos., vol. 17, No.2, pp. 103-136, 2004.

[9] R.J. Goldstein, E.G.R. Eckert and F. Burggraf, "Effects of Hole Geometry and Density on Three-Dimensional Film Cooling", Int. J. Heat. Mass. Tran., vol. 17, pp. 595-607, 1974.

[10] Altuglas International Arkema Inc., Exceptional Grade for Broad-Range Applications. Altuglas International Arkema Inc. 100 PA Rt. 413 Bristol, PA 19007, 2015, www.altuglasint.com

[11] Evonik Industries, PLEXIGLAS® GS/PLEXIGLAS® XT Product Description, Evonik Röhm GmbH, Kirschenallee, 64293 Darmstadt, Germany, 2015, www.evonik.com

[12] Fluent Incorporated (1998a), Gambit: Tutorial Guide, Fluent Incorporated, Lebanon, NH.

[13] Fluent Incorporated (1998b), Gambit: User's Guide, Fluent Incorporated, Lebanon, NH.

[14] Fluent Incorporated (1998c), FLUENT 5 User's Guide, Fluent Incorporated, Lebanon, NH.

[15] Fluent Incorporated (1998d), FLUENT Tutorial Guide, Fluent Incorporated, Lebanon, NH.

[16] B.E. Launder and D.B. Spalding, Lectures in Mathematical Models of Turbulence, Academic Press, London, 1972.

[17] B.E. Launder and D.B. Spalding, "The numerical computation of turbulent flows", Computer Methods in Applied Mechanics and Engineering, vol.3, pp. 269-89, 1974.

[18] C-J. Chen and S-Y. Jaw, Fundamentals of Turbulence Modelling, Taylor & Francis, Washington, DC, 1998.